

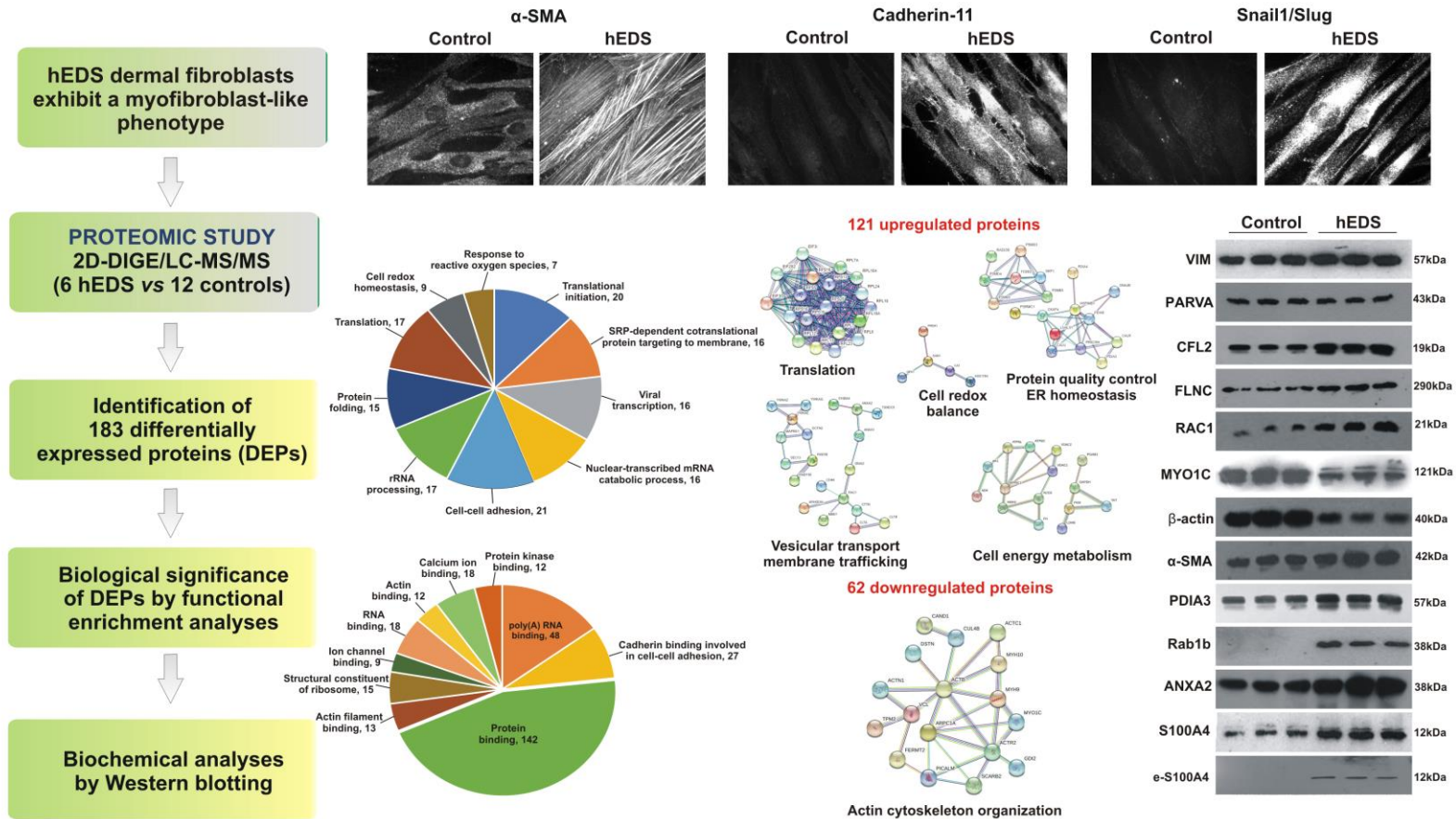
Proteome profiling for hypermobile Ehlers-Danlos syndrome/hypermobility spectrum disorders (hEDS/HSD) to unravel pathogenetic mechanisms and identify potential biomarkers supporting clinical diagnosis

We are very grateful to the Ehlers-Danlos Society for funding this research project aimed to elucidate the intricate protein network and related key molecular pathways that contribute to the pathobiology of hEDS/HSD. Our previous cellular findings revealed that hEDS and HSD patients' dermal fibroblasts undergo a fibroblast-to-myofibroblast transition (FMT), since they exhibit a widespread extracellular matrix (ECM) disarray, including that of collagens (COLLs) and fibronectin (FN), and show a migratory phenotype characterized by α -smooth muscle actin (α -SMA) microfilaments organization, expression of the alternative FN receptor α v β 3 integrin, expression of cadherin-11, and augmented levels of secreted ECM-degrading matrix metalloproteinase 9. We also showed that an α v β 3 integrin-mediated signal transduction pathway, including integrin-linked kinase (ILK) and Snail1/Slug, triggers the FMT. The finding that hEDS/HSD cells exhibit this peculiar myofibroblast-like phenotype, which can be induced in control fibroblasts when treated with hEDS/HSD culture media, is very intriguing, since these highly specialized cells are well-known to contribute to several pathological conditions as they represent an important source of ECM-remodeling enzymes, inflammatory mediators, cytokines, chemokines, and growth factors. Apart from the pathway of the TGF- β 1, the most potent and established stimulator of the FMT, growing evidences on cytoskeleton-dependent signaling and associated mechano-transduction involving integrins and actin remodeling, as well as metabolic alterations and changes in mitochondrial morphology and activity, are emerging. Indeed, during FMT, the actin cytoskeleton regulates not only mechanical functions, but it is also involved in transduction of different signals/stimuli into biochemical signaling and transcriptional and translational regulation. Modifications of cellular metabolism, including ATP generation and synthesis of building blocks are needed to sustain the biomass required for cellular growth and differentiation, as well as the energetic demand of the acquired contractile phenotype. Indeed,

compared with the quiescent state, myofibroblasts increase aerobic glycolysis and lactate production that, in turn, modulate mitochondrial oxidative phosphorylation.

Within the funded project, we continued our previous studies on this peculiar cell model by using 2D-DIGE and LC-MS/MS to compare the cellular proteome of fibroblasts obtained from six patients with hEDS and twelve sex- and age-matched healthy donors. We obtained 183 differentially expressed proteins (DEPs, 121 upregulated and 62 downregulated), and most of them were relevant to biological mechanisms involved in FMT. Indeed, upregulated proteins were mainly involved in cell metabolism, calcium-binding, redox balance, translation, membrane-trafficking, or chaperone function, and downregulated proteins were implicated in actin cytoskeleton remodeling, ECM organization, ER-Golgi trafficking, and lysosomal transport. Our findings, which were recently published in *Biochimica et Biophysica Acta (BBA) - Molecular Basis of Disease* (<https://doi.org/10.1016/j.bbadis.2020.166051>), offer, for the first time, a comprehensive view of dysregulated protein networks and related pathways likely associated with the hEDS pathophysiology. Currently, we are validating some proteome findings on a larger independent cohort of either hEDS or HSD patient cells, also to verify whether these conditions share common specific proteomic signatures and associated pathomechanisms. In the view of an integrative “-omics” approach, we are also engaged in an RNA sequencing project aimed to define possible gene expression changes in hEDS/HSD corroborating our proteome findings. These researches, after targeted *in vivo* translational studies, should offer the possibility to identify disease specific biomarkers defining whether these multisystemic disorders might be part of a phenotypic continuum rather than representing distinct clinical entities and, ultimately, pave the way for the disclosure of therapeutic avenues with a potential benefit for patients’ management.

Novel insights into the molecular mechanisms associated with the pathogenesis of the hypermobile Ehlers-Danlos syndrome (hEDS), orphan of a genetic etiology



**Identification of altered protein networks and potential bioactive molecules
Perspectives for the development of targeted management and therapies**

Summary of the proteome profiling of hEDS patients' dermal myofibroblasts

Six adult females hEDS patients and twelve healthy donors were evaluated at the specialized outpatient clinic for EDS of the University Hospital Spedali Civili of Brescia. Patients were diagnosed according to the 2017 EDS nosology; healthy females were selected with an age range similar to that of patients and by excluding any clinical feature reported in the hEDS nosology as well as several comorbidities associated with the condition. Skin biopsies from patients and healthy donors were established by standard protocol. Before proteome analysis, dermal fibroblasts from all enrolled hEDS patients were evaluated by immunofluorescence microscopy (IF) for the specific myofibroblast-like phenotype (**Figure 1**). All dermal control fibroblasts included in this work were analyzed for the absence of these myofibroblast-like markers as well as for proper organization into the ECM of COLs and expression of their integrin receptor, i.e., the $\alpha2\beta1$ integrin.

Next, the cellular proteome of 6 hEDS myofibroblasts was compared to that of 12 control cells. Qualitative and quantitative differences were assessed by a comprehensive proteomic study based on a combination of two-dimensional difference in-gel electrophoresis (2D-DIGE) followed by matrix-assisted laser desorption/ionization mass spectrometry (MALDI-TOF MS), and label-free liquid chromatography with tandem mass spectrometry label-free (LC-MS/MS). This integrative approach identified 183 differentially expressed proteins (DEPs): 121 were upregulated and 62 downregulated (**Figure 2**).

To obtain an overview of the biological significance of proteomic changes in hEDS myofibroblasts, we performed Gene Ontology (GO) enrichment analysis by using different freely available software packages from DAVID, PANTHER, and STRING biological databases. The proteomic survey of hEDS myofibroblasts revealed significant alterations in different protein classes mainly involved in cellular metabolism and redox homeostasis (19%), cytoskeleton organization (16%), translation (14%), protein modification (8%), membrane trafficking (8%), calcium binding (7%), transport (7%), as well as with chaperone (4%), adaptor (4%), and nucleic acid binding (3%) functions (**Figure 3**).

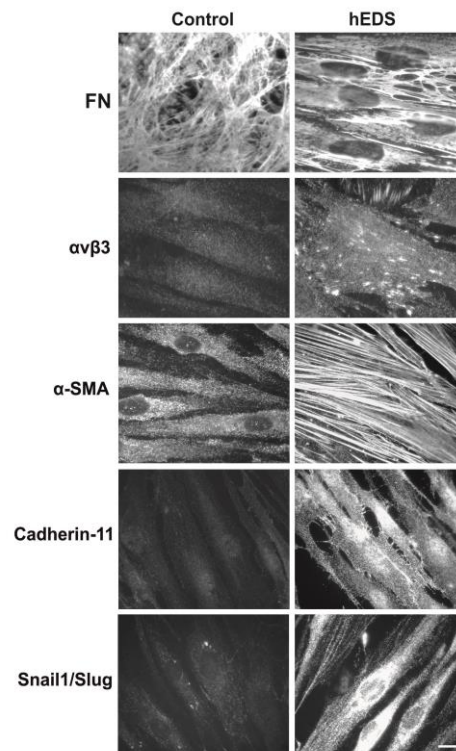


Figure 1. Organization of FN, $\alpha\text{v}\beta\text{3}$ integrin, $\alpha\text{-SMA}$ cytoskeleton, cadherin-11, and Snail1/Slug expression in control and hEDS patient cells. Representative IF analyses of FN-ECM, $\alpha\text{v}\beta\text{3}$ integrin, $\alpha\text{-SMA}$ organization, cadherin-11, and Snail1/Slug distribution in 72 h-grown control and hEDS cells. The organization of $\alpha\text{-SMA}$ and $\alpha\text{v}\beta\text{3}$ integrin as well as the expression of cadherin-11 and Snail1/Slug in hEDS cells are consistent with a myofibroblast-like phenotype. Scale bar: FN, $\alpha\text{-SMA}$, and cadherin-11 9.5 μm ; Scale bar: $\alpha\text{v}\beta\text{3}$ integrin and Snail1/Slug 6 μm .

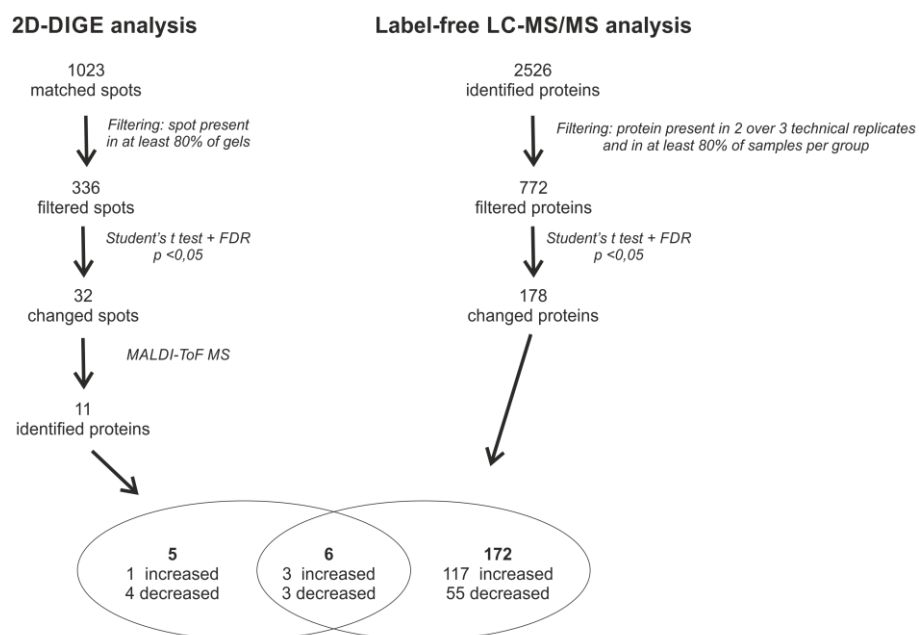


Figure 2. Schematic diagram summarizing identification process and findings obtained from 2D-DIGE and label-free LC-MS/MS proteomic analyses of hEDS vs control cells. 2D-DIGE led to the identification of 11 varied proteins, whereas label-free LC-MS/MS highlighted 178 changed proteins. Of the 6 proteins in common, 3 were increased and 3 decreased in both datasets. False discovery rate (FDR) $p < 0.05$.

Pathways enrichment analysis revealed that “ribosome”, “protein processing in endoplasmic reticulum (ER)”, “carbon metabolism”, “metabolic pathways”, “biosynthesis of amino acids”, “pyruvate metabolism”, and “regulation of actin cytoskeleton” as the most perturbed pathways (Table 1). In particular, pathways implicated in metabolic processes, protein translation and processing into the ER lumen, and maintenance of ER proteostasis seem to be enhanced, as suggested by the increased expression of numerous associated proteins. Molecular functions involved in focal adhesion/cell-matrix interactions and fibroblast-specific actin cytoskeleton organization seem to be impaired, given the differential expression of several related proteins, the majority of which were downregulated.

GO enrichment analysis and protein-protein interaction networks indicated that the 121 upregulated proteins were mainly involved in cell metabolism (e.g. ATP5O, ATP5C1, ATP5L, ACO2, MDH2, FH, ACADVL, ECHS1, HADHB, ETFA, ADK, AK1, VDAC1, VDAC2, NME1, NAGK, GAPDH, PGAM1, PKM, TKT, LDHB), calcium-binding (CALM1, CALM2, CALU, S100A4, S100A13, RCN3, ANXA1, ANXA2, ANXA7), redox balance (SOD1, CAT, GPX1, PRDX1, PRDX3, PRDX5, GSTP1, HSP90B1), translation (e.g. RPL23, RPS5, RPL12, RPL10A, EIF2S2, EIF3I, EIF3G, RPL24, etc.), membrane-trafficking and/or chaperone function (e.g. TXNDC5, CD44, RAC1, CTTN, TBCA, CALR, BAG2, HSPE1, HSP90B1, FKBP1B, CLTA, CLTB, NME1, RAB1B, SEC13, MAPRE1, DCTN2, STX7).

The 62 downregulated proteins were mainly implicated in actin cytoskeleton organization (e.g. CAND1, CUL4B, DSTN, ACTC1, ACTN1, VCL, ACTB, MYH9, MYH10, MYO1C, TPM2, FERMT2, ARPC1A, PICALM, SCARB2, GDI2, ACTR2), lysosomal transport (LAMP1, LAMP2), tRNA aminoacylation (QARS, LARS, AARS), ECM organization (COL1A1, COL6A2), and ER-Golgi trafficking (USO1, COPE) (**Figure 4**).

Table 1. Most significantly perturbed pathways in hEDS myofibroblasts according to the STRING database

KEGG ID	Pathway description	Count	FDR	Proteins in the pathway
hsa03010	Ribosome	16	7,16E-11	RPL18, RPL13, RPL24, RPS5, RPS25, RPS18, RPS19, RPS16, RPL7, RPL23, RPL18A, RPL6, RPS13, RPL7A, RPL12, RPL10A
hsa04141	Protein processing in endoplasmic reticulum	14	7,77E-08	BAG2, CALR, CKAP4, DNAJB11, HSP90B1, PDIA3, PDIA4, PDIA6, PRKCSH, RAD23B, SEC13, SKP1, TXNDC5, CRYAB
hsa01200	Carbon metabolism	10	1,58E-05	ACO2, CAT, PKM, ECHS1, FH, GAPDH, MDH2, PFKP, PGAM1, TKT
hsa01230	Biosynthesis of amino acids	7	0,00039	ACO2, GAPDH, MAT2A, PKM, PGAM1, PFKP, TKT
hsa05016	Huntington's disease	10	0,00071	ATP5C1, ATP50, CLTA, CLTB, DCTN2, GPX1, SOD1, TGM2, VDAC1, VDAC2
hsa01100	Metabolic pathways	27	0,0012	ACADVL, ACO2, ADK, AK1, ATP5C1, ATP5L, ATP50, CBR1, ECHS1, FH, GAPDH, GLS, HADHB, HSD17B4, LDHB, MAT2A, MDH2, NAGK, NME1, NNMT, P4HA2, PFKP, PGAM1, QARS, SRM, TKT, UGDH
hsa04510	Focal adhesion	9	0,0029	VCL, COL1A1, ITGA5, COL6A2, FLNC, PARVA, RAC1, FLNA, ACTN1
hsa04810	Regulation of actin cytoskeleton	9	0,0035	VCL, MYH9, ARPC1A, ITGA5, CFL2, RAC1, MYH10, ACTN1, CFL1
hsa00620	Pyruvate metabolism	4	0,0096	PKM, MDH2, FH, LDHB

Proteins with an increased expression are highlighted in bold.

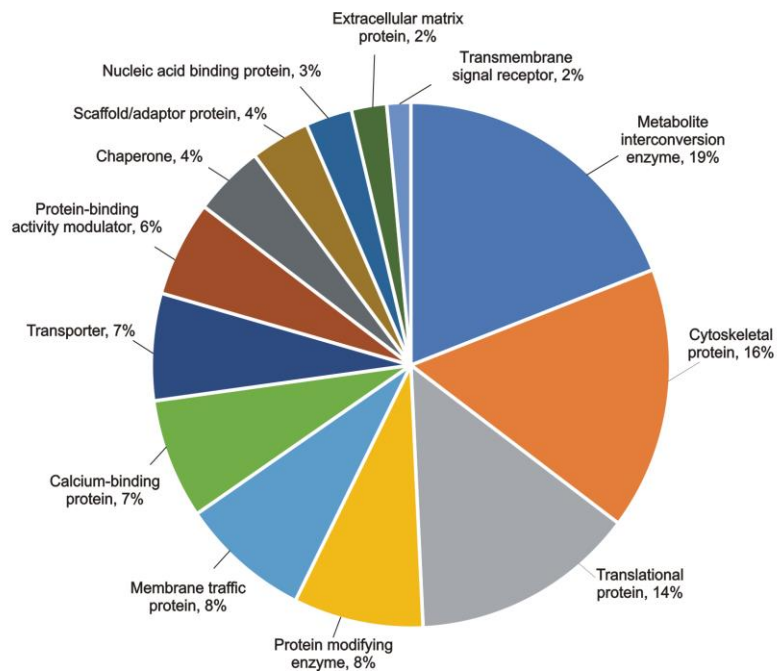


Figure 3. Overview of the main altered protein classes in hEDS dermal myfibroblasts according to the PANTHER database.

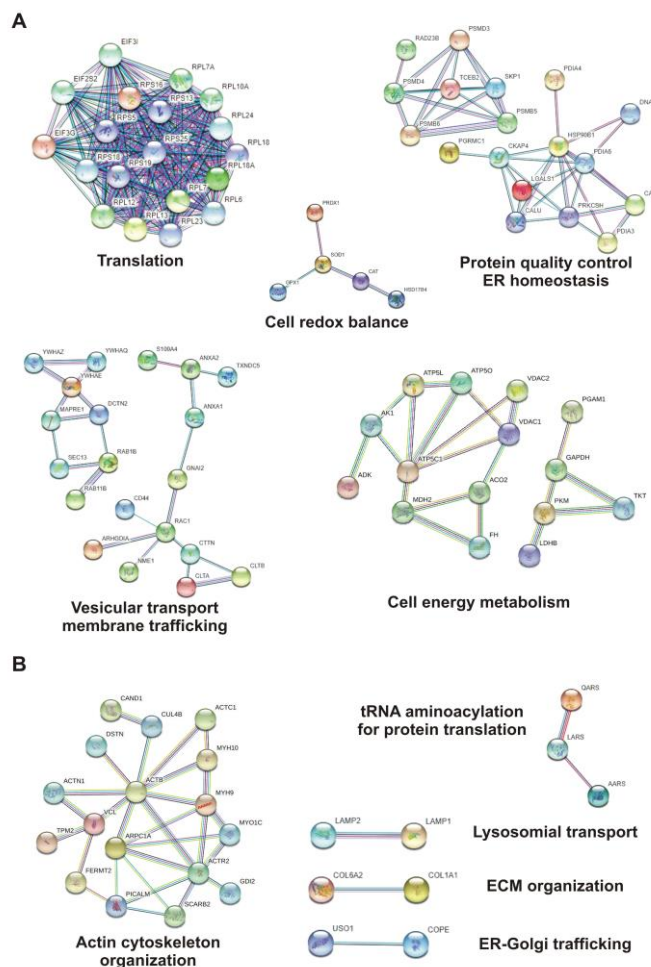


Figure 4. Most significant protein-protein interaction networks of up- (A) and downregulated (B) proteins identified in hEDS myfibroblasts based on the STRING database. Each node represents a protein, and each edge represents an interaction including either physical or functional associations.

We confirmed the differential expression by performing Western Blotting and IF of subset of proteins related to different cellular pathways, i.e., cytoskeleton organization [vimentin (VIM), cofilin 2 (CFL2), α -parvin (PARVA), filamin C (FLNC), Rac family small GTPase 1 (RAC1), myosin IC (MYO1C), β -actin, α -SMA], intracellular trafficking/vesicular transport and cell redox homeostasis [protein disulfide isomerase family A member 3 (PDIA3), member RAS oncogene (Rab1b), annexin 2 (ANXA2), and either the intracellular family S100 calcium binding protein A4 (S100A4) or the extracellular fraction secreted through microvesicles (e-S100A4)] (**Figure 5**).

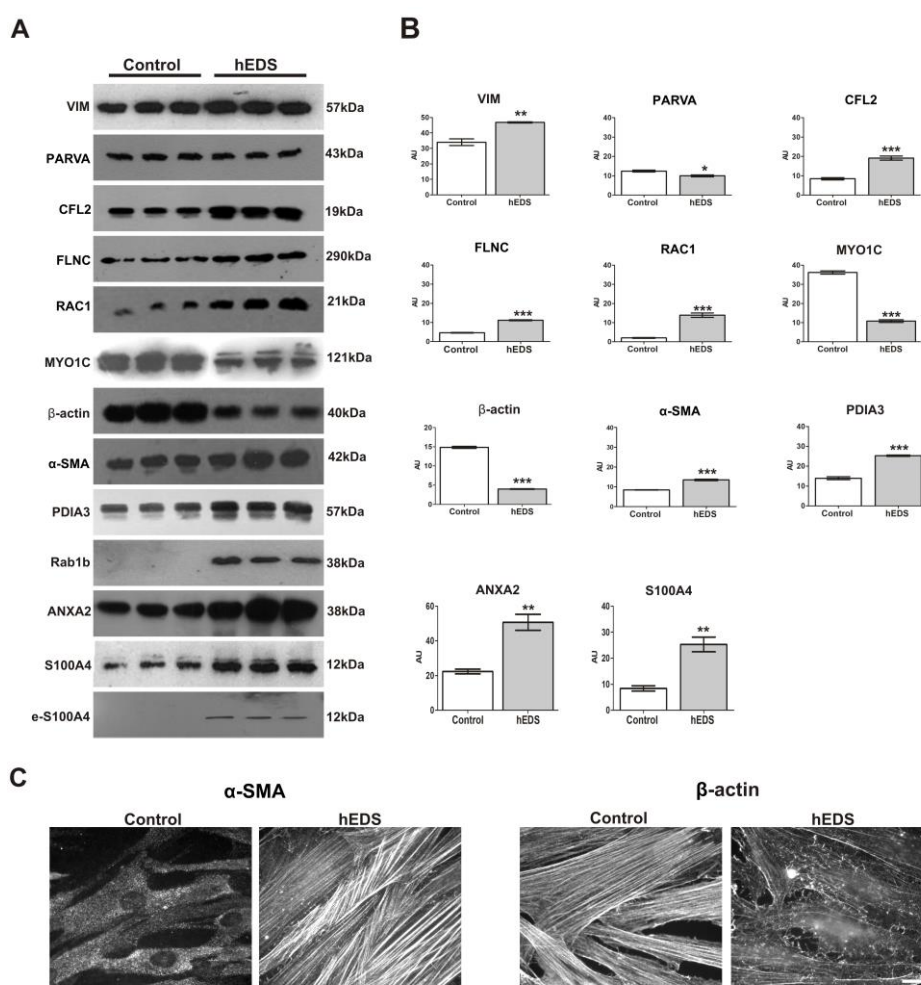


Figure 5. Representative Western blotting images (**A**) and respective quantitative analyses (**B**) of protein amounts in pooled whole cell extracts from control fibroblasts (n=6, white bars) and hEDS myofibroblasts (n=6, gray bars) of VIM, PARVA, CFL2, FLNC, RAC1, MYO1C, β -actin, α -SMA, PDIA3, Rab1b, ANXA2, and S100A4. This latter was also analyzed in pooled CM of control and patient cells, starting from 100 μ g of proteins recovered after a specific lysis treatment and immunoreacted with the mouse S100A4 mAb, detecting a 12 kDa band (e-S100A4) only in the culture media of hEDS myofibroblasts. Protein bands were quantified by image analysis and IOD values were normalized against the total amount of loaded proteins stained with Sypro Ruby Protein Blot Stain. Representative IF analyses (**C**) of α -SMA and β -actin cytoskeleton organization in control and hEDS cells. Scale bar: 9.5 μ m. All graphical results are expressed as mean \pm SEM of technical triplicates. Statistical analysis was performed with the Student's t-test. * $p < 0.05$, ** $p < 0.01$, *** $p < 0.001$.